



**GEOLOGICAL SURVEY OF CANADA
OPEN FILE 7045**

**A geostatistical approach for two-dimensional seismic velocity
modelling**

M. Claprood, M.J. Duchesne and E. Gloaguen

2011



Natural Resources
Canada

Ressources naturelles
Canada

Canada



**GEOLOGICAL SURVEY OF CANADA
OPEN FILE 7045**

**A geostatistical approach for two-dimensional seismic velocity
modelling**

M. Claprood¹, M.J. Duchesne^{2,1}, and E. Gloaguen¹

1. Institut National de la Recherche Scientifique, Centre Eau-Terre-Environnement, Québec, Canada
2. Geological Survey of Canada, Québec, Canada.

2011

©Her Majesty the Queen in Right of Canada 2011

doi:10.4095/289551

This publication is available from the Geological Survey of Canada Bookstore (http://gsc.nrcan.gc.ca/bookstore_e.php). It can also be downloaded free of charge from GeoPub (<http://geopub.nrcan.gc.ca/>).

Recommended citation:

Claprood, M., Duchesne, M.J., and Gloaguen, E., 2011. A geostatistical approach for two-dimensional seismic velocity modelling; Geological Survey of Canada, Open File 7045, 21 p. doi:10.4095/289551

Publications in this series have not been edited; they are released as submitted by the author.

ABSTRACT

This study tests two geostatistical approaches, kriging with external drift (KED) and cokriging (CK), for building two-dimensional seismic velocity models for the reprocessing of vintage seismic reflection data collected in Canadian Western Arctic Islands between the late 1960s and the early 1980s. The interval thickness between horizons is estimated at all Common Mid Points (CMPs). The interval thickness evaluated at three wells is used as the primary variable of kriging and the time-thickness estimated from seismic horizon picking at all CMPs is used as the external drift to represent time-depth variations along the seismic line. The depth to horizons estimated by KED honours perfectly the depth evaluated at three wells, while the lateral variations of the horizons in depth closely follow those of the horizons picked in time-depth. In contrast to constant lateral velocity layer models often used in seismic processing, the velocity calculated from the KED allow modelling lateral velocity variations within each layers, providing a more realistic representation of the subsurface geology.

INTRODUCTION

One of the key aspects in seismic processing is the availability of robust velocity models to generate subsurface images that are geologically realistic and meaningful. This study applies and adapts geostatistical methods for building two-dimensional (2-D) seismic velocity models. The models are used to reprocess seismic reflection data collected on Sabine Peninsula (Canadian Western Arctic Islands) between the late 1960s and the early 1980s. The reprocessing of this vintage seismic dataset will be used to support the hydrocarbon resource evaluation of the Western Arctic Islands that has been undertaken by the Geomapping for Energy and Minerals program (2008-2013) of the Geological Survey of Canada.

In this study, we apply two existing geostatistical methods, kriging with external drift (KED) and cokriging (CK) to generate seismic velocity models for seismic line 2674. These two methods were adapted to the available data sets detailed in the next section. Line 2674 was selected to test both approaches since 1) it crosses most of the peninsula in a N-S fashion and thus geological layers are believed to be affected by significant lateral changes of velocity, 2) three relatively deep (5408 to 5450 m) wells were drilled along the line and 3) for comparison purposes as the line was also migrated at the Department of Physics of the University of Alberta using a different velocity model (Figure 1; Kanasewich and Berkes, 1988). Results obtained are also compared with a layered Earth model

formed by constant RMS velocity layers which were determined from averaged RMS velocity values computed on well logs (Figure 2).

The Sabine Peninsula is located on Melville Island on the fringe of the Sverdrup Basin in the Queen Elizabeth Islands of the Western Arctic (Figure 1). Between 1961 and 1985, 22 wells were drilled and >3400 line-km of seismic reflection data were acquired on Sabine Peninsula. The stratigraphic section includes the Franklinian (Precambrian to Upper Devonian) and the Sverdrup (Pennsylvanian to Early Tertiary) successions (Goodbody and Christie, 1993; Harrison, 1995). The Franklinian succession is composed by folded strata of limestone, shales and sandstones. However this succession remains widely unknown on Sabine peninsula as it was only sampled by 1 of the 22 wells drilled, this well being the southernmost. The Sverdrup succession is formed of slightly deformed Triassic to Cretaceous aged sandstone, siltstone, and minor amounts of carbonate. Deformed evaporitic rocks are exposed in two piercement diapirs on northern Sabine Peninsula – the Barrow and Colquhoun domes.

DATA SETS

Line 2674 was collected by United Geophysical for Panarctic Oils Ltd. in 1981 using ~23 kg dynamite charges as seismic sources and a 6432 m-long spread composed of 96 channels as a recording system. The line is ~67 km long and was recorded to 6 seconds. Seismic horizon picks, sonic logs and time-depth (TD) conversion charts derived from check shots are used to build the velocity models. Five horizons were identified and picked on a stacked version of line 2674 based the coherency and the amplitude of the reflections along the line (Figure 2). Horizons were traced semi-automatically and edited manually on the seismic section. Sonic logs and check shots from wells F-34, K-71, and D-68 were projected onto Common-Mid-Points (CMP) 631, 1047, and 1404, respectively (Figure 2).

In the initial layered Earth model used to reprocess line 2674, constant RMS velocities were computed from averaged interval velocities within each layer of the model. However, as seen in figure 2, the RMS velocities calculated from wells logs for each horizon interval show some lateral variability within each layer. Consequently, the constant RMS velocity layer model used to initially reprocess the seismic line is not representative of the lateral velocity variations within each layer. Accurate velocity models are important to adequately represent the lateral and vertical variations of velocity (Viloria et al., 2009). Geostatistical methods such as kriging are adapted to optimize the information available. Many studies have applied geostatistical methods with success to derive velocity models or estimate reservoir properties. For example, Hwang and McCorkindale (1994) found KED to be an effective tool

to provide reliable averaged velocity of the Troll Field (North Sea). Collocated cokriging was used by Lamy et al. (1998) for transforming impedances into reservoir parameters. More recently, Claprood et al. (submitted) successfully used KED to build a 3D structural model of the St. Lawrence Lowlands in the Bécancour area, Québec, Canada. A similar methodology is applied in this study, by conjointly using depth and travel time horizon information to estimate the most reliable velocity model of line 2674.

METHODOLOGY

Kriging is a deterministic geostatistical approach to provide unbiased solution by minimizing the estimation variance. It is used to interpolate a variable using a set of scattered data points (Dubrule, 2003). We express the equation of simple kriging as:

$$Z_{uk}(x_0) = m_z + \sum_{i=1}^N \lambda_i (Z(x_i) - m_z), \quad (1)$$

where Z is the variable at all known points x_i ; m_z is the mean of the variable Z ; λ_i are the kriging weights to estimate; and Z_{uk} is the variable to estimate at points x_0 (Doyen, 2007).

When the primary variable Z is not known at a sufficient number of data points, it is advantageous to use information from an alternate source to improve the estimation. In this study, we want to estimate the interval thickness between all horizons identified on line 2674 at all CMPs, using the depth intervals evaluated at three wells located at offsets 20.94 km, 34.84 km, and 46.76 km. The use of 3 data points is not sufficient to compute adequate statistics to employ simple kriging. Thus two methods are considered to include time-depths of 5 horizons picked on the seismic line along with well data in the kriging process: kriging with external drift and cokriging.

Kriging with external drift

The KED scheme has been designed for seismic applications, particularly for time to depth conversion (Dubrule, 2003) as it is the case in this study. KED is easily adapted from single kriging by replacing the mean m_z from equation (1) by a function (external drift T_x) expressing the spatial variations of the seismic horizons as $m_z = a + bT_x$.

In this study, the time-depth of the seismic interval estimated from seismic picks at all CMPs is used as the external drift to represent the variations in interval thicknesses along the 5 horizons. The kriging process ensures that the interval thicknesses delimited by the horizons measured at the three wells is perfectly respected.

Cokriging

CK uses the relation between the primary variable (interval thickness) and a secondary variable (time-intervals derived from seismic horizons) to improve the estimation. The CK equation is expressed as:

$$Z_{uk}(x_0) = m_Z + \sum_{i=1}^N \lambda_i (Z(x_i) - m_Z) + \sum_{j=1}^M w_j (Y(x_j) - m_Y), \quad (2)$$

where $Y(x_j)$ is the secondary variable known at points j , m_Y is the mean of the variable Z_Y ; λ_j are the cokriging weights to estimate. Conversely to KED, the cokriging process assumes that a linear relation is known between the primary and secondary variables, a relation which is taken into account by the use of the cross-covariance between the two variables in the kriging scheme.

The KED and CK methods are used to estimate the interval thicknesses sequentially from the top to the bottom horizons. They are first used to estimate the depth of the shallowest horizons, using the depth to horizon estimated at three wells as the primary variable, and considering the travel time seismic picks of the first horizon at all CMPs of seismic line 2674 as the external drift (for KED) or the secondary variable (for CK). For all four remaining horizons, the interval thickness is used as the primary variable of kriging, and time-depth picks of each horizon is considered as the external drift or secondary variable to guide the estimation away from the three wells where the primary variable (depth) is known.

For each horizon, the first step is to compute the experimental variogram on the primary variable. Since the primary variable is known at an insufficient number of CMPs (i.e. 3 CMPs corresponding to 3 projected well locations), the variograms are computed from the seismic horizon picks in time-depth. The time-depths of the picks are rescaled so they best represent the true mean and variance of the intervals in thickness. Experimental variograms computed from the shallowest (horizon 5, Figure 2) to the deepest horizon (horizon 1, Figure 2) are presented in figure 3, along with their best-fit modeled variograms. Modeled variograms are graphically adjusted so they best represent the variation of the variogram to a first plateau where the experimental variogram stays at a constant value or falls back.

The plateau is referred as the sill (c) and represents the variance of the interval thickness. The sill is reached at a distance known as the range (a), with a variogram structure defined as spherical, exponential or gaussian model. The structure of the variogram defines the level of smoothness of the kriged variable for distances smaller than the range for which the modeled variogram is used to represent the variations of the primary variable. At distance greater than the range, all variations of the kriged interval thickness with position are represented by the seismic horizon picked in time-depth.

Seismic velocity calculation

Once the interval thicknesses delimited by different horizons have been kriged, the depth to each horizon is computed. Three different seismic velocity fields (interval velocity (v_{int}), RMS velocity (v_{rms}), and average velocity (v_{ave})) are computed from the following equations:

$$v_{int} = 2 \frac{\Delta z_i}{\Delta \tau_i}, \quad (3)$$

$$v_{rms} = \sqrt{\frac{1}{t_0} \sum_{i=1}^N v_i^2 \Delta \tau_i}, \quad (4)$$

$$v_{ave} = \frac{1}{t_0} \sum_{i=1}^N v_i \Delta \tau_i, \quad (5)$$

where Δz is the depth interval of each horizon i , $\Delta \tau$ is the time-distance interval of each horizon, N is the total number of horizons, and $t_0 = \sum_{i=1}^N \Delta \tau_i$ the sum of time-depth interval (Yilmaz, 2001).

RESULTS

Velocity Field from Kriging with External Drift

The depth to all horizons estimated by KED is presented in figure 4b. The plot clearly shows that the depth to horizons estimated by KED honours the depth evaluated from check shots at the 3 well locations projected on line 2674 respectively at offsets 20.94 km, 34.84 km, and 46.76 km. The variations of the horizons in depth closely follow those of the horizon picks in time-depth, as expected when using the KED scheme. The kriged horizons in depth and picked in time-depth are then used to compute v_{int} , v_{rms} and v_{ave} .

Time-distance plots of the velocity fields obtained by KED are presented in figure 5. The velocity is assumed to have no vertical variations within a specific layer, as only lateral variations are evaluated by KED.

Comparisons between the three seismic velocity fields calculated are shown in figure 6 using difference plots. Since there is a fundamental difference in the definition of interval velocity compared to the RMS and average velocities, important differences were expected and are observed in figure 6. Those differences increase with depth, where the averaging used in the computation of RMS and average velocities has a greater impact on the resulting velocities computed. RMS velocity values are up to 10% larger than average velocity values computed at all CMPs. The difference of a few percents between RMS and average velocity values is well documented in the literature and thus was anticipated in this study (see Sheriff and Geldart, 1995).

Velocity Field from Cokriging

The main difference between KED and CK is how the secondary variable is taken into account in the estimation process. While it replaces the mean (m_z in equation 1) in the KED scheme, it is used to minimize the kriging weights by adapting equation 1 to form the cokriging scheme (equation 2). Solving the cokriging system implies knowing and quantifying the relation between the primary and secondary variables through a covariance. Since the primary variable (interval thickness) is known at a maximum of three points only (i.e. the wells), the covariance can not be known with precision. Arbitrary coefficients of correlation of 0.8 and 0.9 have been input in the cokriging scheme. The value of these coefficients has been determined to be high enough to represent a strong correlation between the two variables, but the exact value has no physical meaning.

Cokriging has been tested first on the time picks of horizon 4. The results from CK are presented in figure 7, along with a comparison with the results obtained by KED for the same time picks. As expected from any kriging schemes, the kriged time picks agree perfectly with the observed thickness at all three well locations. We observe similar trends between the time picks estimated by KED and CK. There is a noticeable difference between the results obtained by cokriging when using different coefficients of correlation between the primary and secondary variables. The choice of the coefficient of correlation cannot be justified by any observation or parameters, since only three points are available to estimate this correlation, generating high variability in the results obtained by CK. As

mentioned by Hirsche et al. (1998), the initial assumptions underlying the use of geostatistics are of prime importance as they can lead to false results if these assumptions are incorrect. The cokriging option was thus judged unreliable to model a representative seismic velocity field considering the limited number of wells located along line 2674 from which true interval thicknesses are measured.

Initial reprocessing results

For assessing the performance of the developed approach, the original stack version of line 2674 was migrated using the post-stack Kirchhoff method in the time domain (Figure 9; Schneider, 1978). Results obtained are compared to a version of line 2674 migrated using a constant velocity layer model (Figures 8a and 9). For both migrations the same aperture and angle parameters were used, and thus only the RMS velocity model differed. The deepest part of the original stack section is dominated by hyperbolic reflections attributed to steeply dipping reflectors that are inadequately sampled spatially (Claerbout, 1993). Both migrations have successfully collapsed hyperbolic reflections except the hyperbola denoted by the black arrow that most likely correspond to sideswipes correlative to steep structural features lying out of the vertical plane of the survey line. However the image migrated with the constant velocity layer model presents numerous migration “smiles” (indicated by the white arrows on figure 9c) that are diagnostic of data that have been migrated using inadequately high seismic velocities (Zhu et al., 1997). Those migration artefacts are not present on the seismic image obtained with the KED velocity model (Figures 6b, 8b and 9d).

Additionally, the migrated image achieved by the KED velocity model is compared to a version of the same line processed by Kanasewich and Berkes (1988) for which they used a velocity model constructed from 3 velocity analyses (figure 9b). Results of both migrations are equivalent although they used 1) a stack version of the line that benefited from a more advanced pre-stack processing flow than the stack section that we had access to and 2) a finite-difference migration approach instead of a Kirchhoff migration scheme (figure 9). Finally, some residual low amplitude migration “smiles” are present on the migrated section of Kanasewich and Berkes (1988) (see white arrows on figure 9b).

DISCUSSION

The velocity model obtained by KED (Figure 5) respects the lateral variations in time-depth imposed by the picked horizons. Also it shows lateral velocity changes within each layer which are more

realistic than assuming no lateral changes. Lateral velocity variations within each geological layer are generally expected in the subsurface and observed at different scales (Røste et al. 2006; Tiwary et al. 2009). Moreover the importance of the lateral velocity changes within a single geological layer is expected to be even more significant for seismic lines covering longer distances such as line 2674. This statement is supported by comparisons between the migrated image of line 2674 using a constant velocity layer model and the KED velocity model (Figure 9).

Further comparisons are made between the velocity model built by KED and a constant velocity model having the same layering (i.e. derived from horizon picking) that was constructed by averaging RMS velocities from the sonic logs of the 3 wells projected on line 2674 (Figures 2 and 8). We clearly observe the lateral variations of the difference between KED estimated and constant velocity models, especially in the two shallowest horizons. The estimation of RMS velocity by KED seems to underestimate the RMS velocity computed from well logs in the deepest horizons. This is not related to the KED procedure, but more likely to the scale difference between the velocity computed from sonic logs used in the constant velocity model and the time-to-depth relationship evaluated by check shot surveys at the selected CMPs used in the velocity model generated by KED (Figure 8).

CONCLUSIONS

Five main conclusions are drawn for this study:

1. The seismic horizons picked in time-depth are believed to be correlative with variations in depth of the geological units and thus can be considered to build a representative velocity models.
2. Kriging with external drift is more accurate than cokriging to estimate the depth of horizons when insufficient data points are available to compute adequate statistics.
3. Velocity estimated by KED closely matches the velocity estimated at 3 wells from time-depth conversion derived from check shot surveys.
4. Velocity models estimated by KED show lateral variations which are more representative of the subsurface velocity than constant velocity layers traditionally used.
5. Reprocessing, and more specifically migration, benefited from using a model that includes lateral changes of velocity within each layer.

The use of kriging with external drift is thus recommended to evaluate realistic velocity models along seismic lines where time-depth conversion is known at limited CMPs, as demonstrated in this study.

ACKNOWLEDGEMENTS

Authors are grateful to Suncoar for giving access to seismic line 2674. Jim Dietrich (GSC-Calgary) is acknowledged for reviewing this contribution. This study was supported by the Western Arctic Islands Geomapping for Energy and Minerals project.

REFERENCES

- Claerbout, J. (1993) Earth sounding analysis: processing versus inversion. Blackwell Scientific Publications, Cambridge, UK.
- Claprood, M., Gloaguen, E., Giroux, B., Duchesne, M., Konstantinovskaya, E., Malo, M., and Massé, L., Deep saline aquifer structural characterization for CO₂ storage – A case study in the St. Lawrence Lowlands, Canada, submitted to the International Journal of Greenhouse Gas Control.
- Doyen, P. (2007) Seismic Reservoir Characterization, An Earth Modelling Perspective. Education Tour Series, EAGE Publications bv, Houten, The Netherlands, sponsored by the European Association of Geoscientists & Engineers.
- Dubrule, O. (2003) Geostatistics for seismic data integration in earth models. Distinguished Instructor Series, No.6, Society of Exploration Geophysicists, Tulsa, USA, sponsored by the Society of Exploration Geophysicist and the European Association of Geoscientists & Engineers
- Goodbody, Q.H. and Christie, R.L. (1993) Summary of stratigraphy of Melville Island, Arctic Canada. *In* The Geology of Melville Island, Arctic Canada, R.L. Christie and N.J. McMillan (eds.). Geological Survey of Canada, Bulletin 450: 13-22.
- Harrison, J.C. (1995) Melville Island's salt-based fold belt, Arctic Canada. Geological Survey of Canada, Bulletin 472, 344 pages.
- Hirsche, K., Boerner, S., Kalkomey, C., and Gastaldi, C. (1998) Avoiding pitfalls in geostatistical reservoir characterization: A survival guide. The Leading Edge, 17: 493-504.
- Hwang, L.F. and McCorkindale, D. (1994) Troll field depth conversion using geostatistically derived average velocities. The Leading Edge, 13: 262-269.
- Kanasewich, E.R. and Berkes, Z. (1988) Reprocessed and interpreted seismic reflection data from the Arctic platform, Parry Islands fold belt, and the Sverdrup basin on Eastern Melville Island, Canadian Arctic Islands. Geological Survey of Canada, Open File 1818, 32 pages.
- Lamy, P., Swaby, P., Rowbotham, P., and Dubrule, O. (1998) From seismic to reservoir properties using geostatistical inversion, *in*: SPE Annual Technical Conference and Exhibition, Society of Petroleum Engineers, New Orleans, Louisiana, USA: 69-79.

- Røste, T., Stovas, A. and Landrø, M. (2006) Estimation of layer thickness and velocity changes using 4D prestack seismic data. *Geophysics*, 71: S219-S-234.
- Schneider, W.A. (1978) Integral formulation for migration in two and three dimensions. *Geophysics*, 43: 49-76.
- Sheriff, R.E and Geldart, L.P. (1995) *Exploration Seismology*. Cambridge University Press, New York, USA.
- Tiwary, D.K., Bayuk, I.O., Vikhorev, A.A. and Chesnokov, E.M. (2009) Comparison of seismic upscaling methods: from sonic to seismic. *Geophysics*, 74: WA3-WA14.
- Vilorio, R., Garcia, I., Caudron, A., Cariel, R., De Caires, F., Hernandez, J., and Bustos, A. (2009) Using a fine-tuned interval velocity model for improving the quality of time-to-depth conversion. *The Leading Edge*, 28: 1430-1434.
- Yilmaz, O. (2001) *Seismic data analysis: Processing, inversion and interpretation of seismic data*. Investigations in Geophysics, No.10, Society of Exploration Geophysics, Tulsa, USA.
- Zhu, J., Lines, L.L. and Gray, S.H. (1997) Smiles and frowns in migration/velocity analysis. CREWES Research Report, 9: 33-1-33-21.

FIGURES

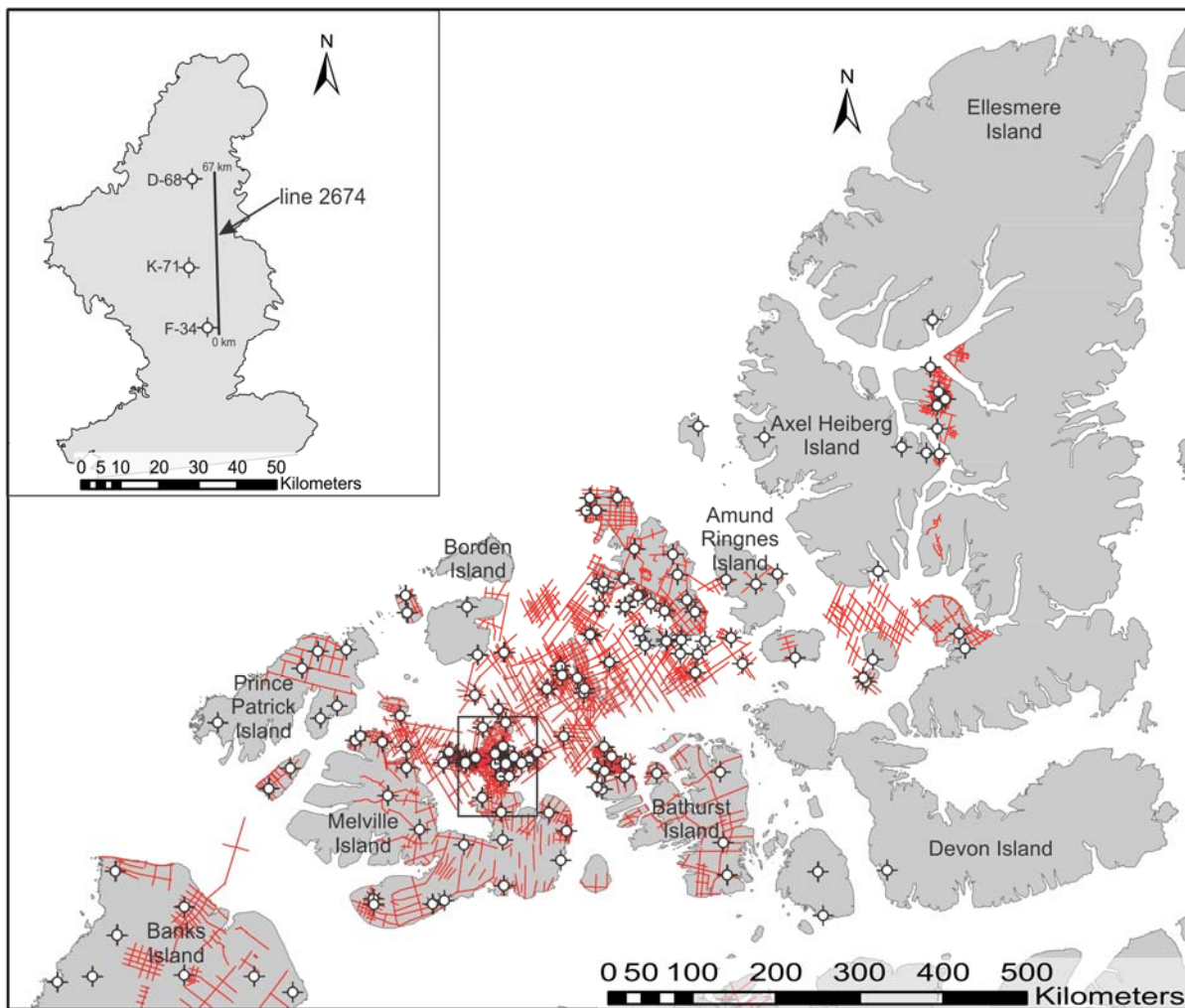


Figure 1. Distribution of seismic and well data coverage in the Canadian western Arctic. The inset of Sabine Peninsula indicates location of seismic line and wells used in this study.

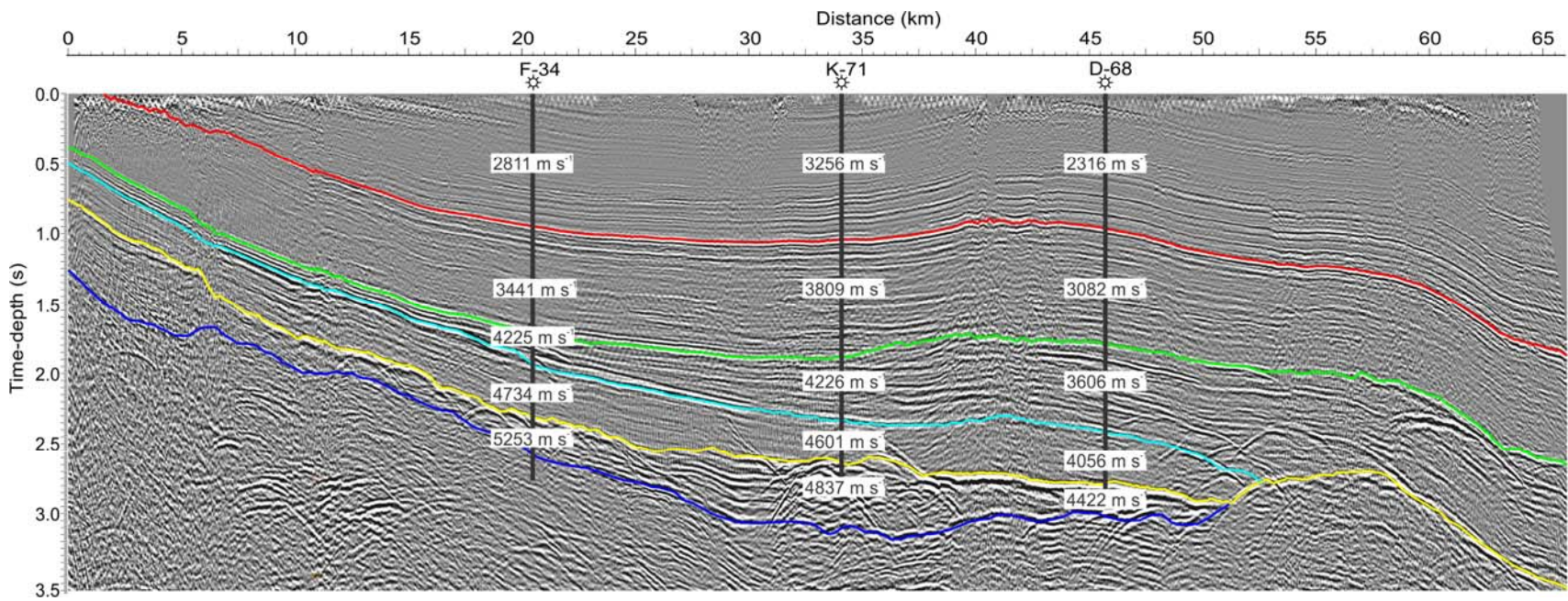


Figure 2. 0 to 3.5 s time-window of original stack section 2674. The horizon picks, the projected subsurface location of the wells and the RMS velocities calculated from well logs for each horizon interval are plotted on the section. The dashed-line rectangle shows location of figure 9.

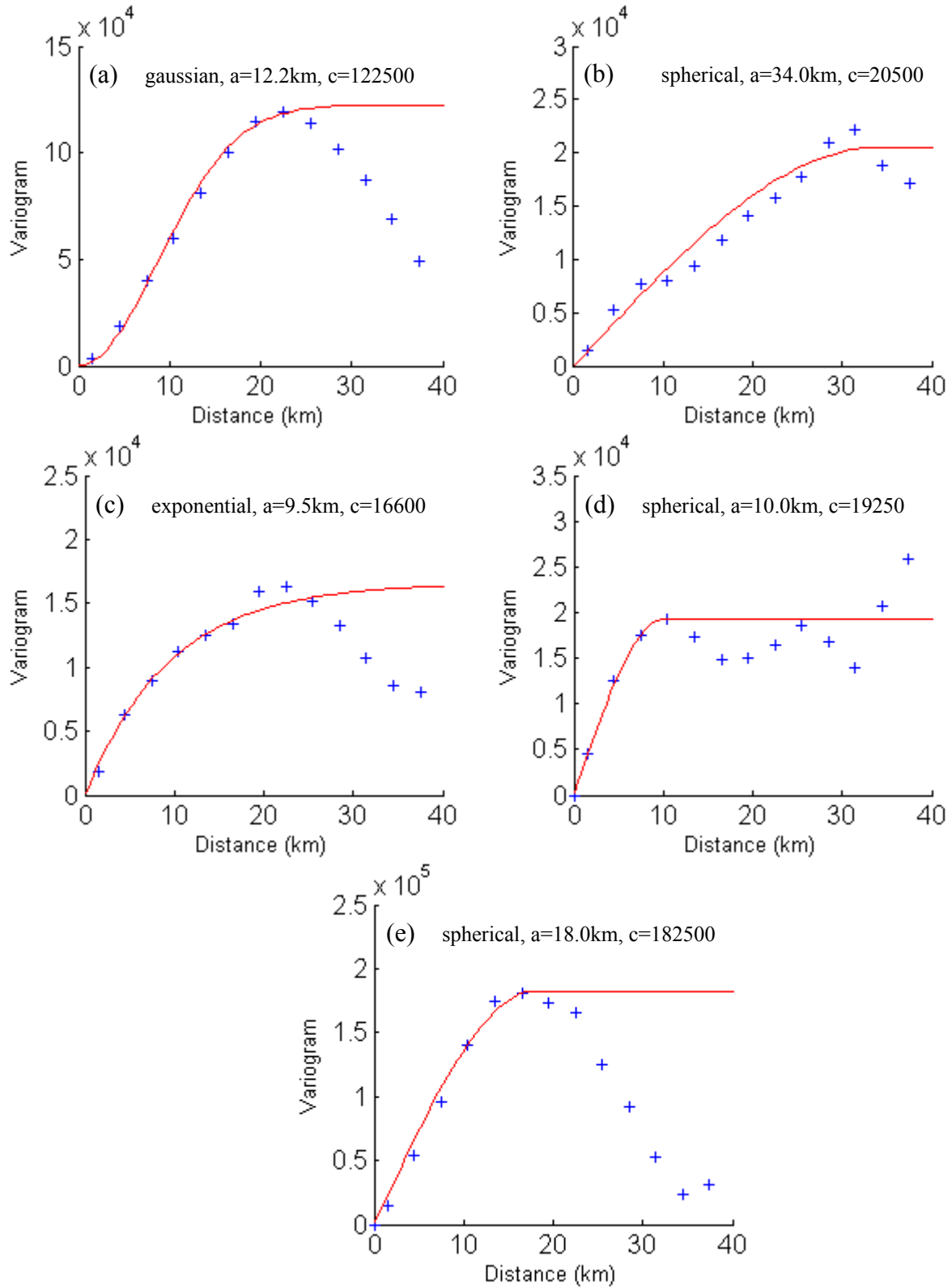


Figure 3. Experimental (blue crosses) and modeled (red curve) variograms computed from the time-depths of (a) the shallowest to (e) the deepest horizons.

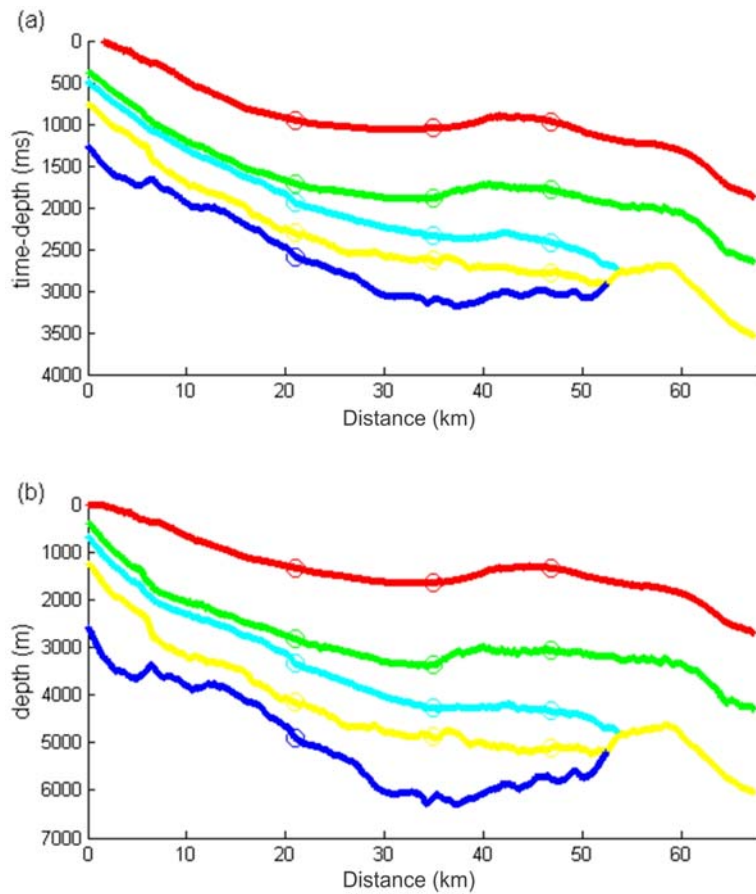


Figure 4. (a) Seismic horizons picked in time-depth on the original stack section 2674, (b) Kriged depth to horizon estimated by KED. For each horizon, time-depth pairs obtained from checkshot surveys made at the 3 wells are illustrated by open circles. Notice that the kriged horizons in depth precisely honours the depth measured at all three CMPs. The horizon variations in depth along distance follow the time-depth variations interpreted by horizon picking.

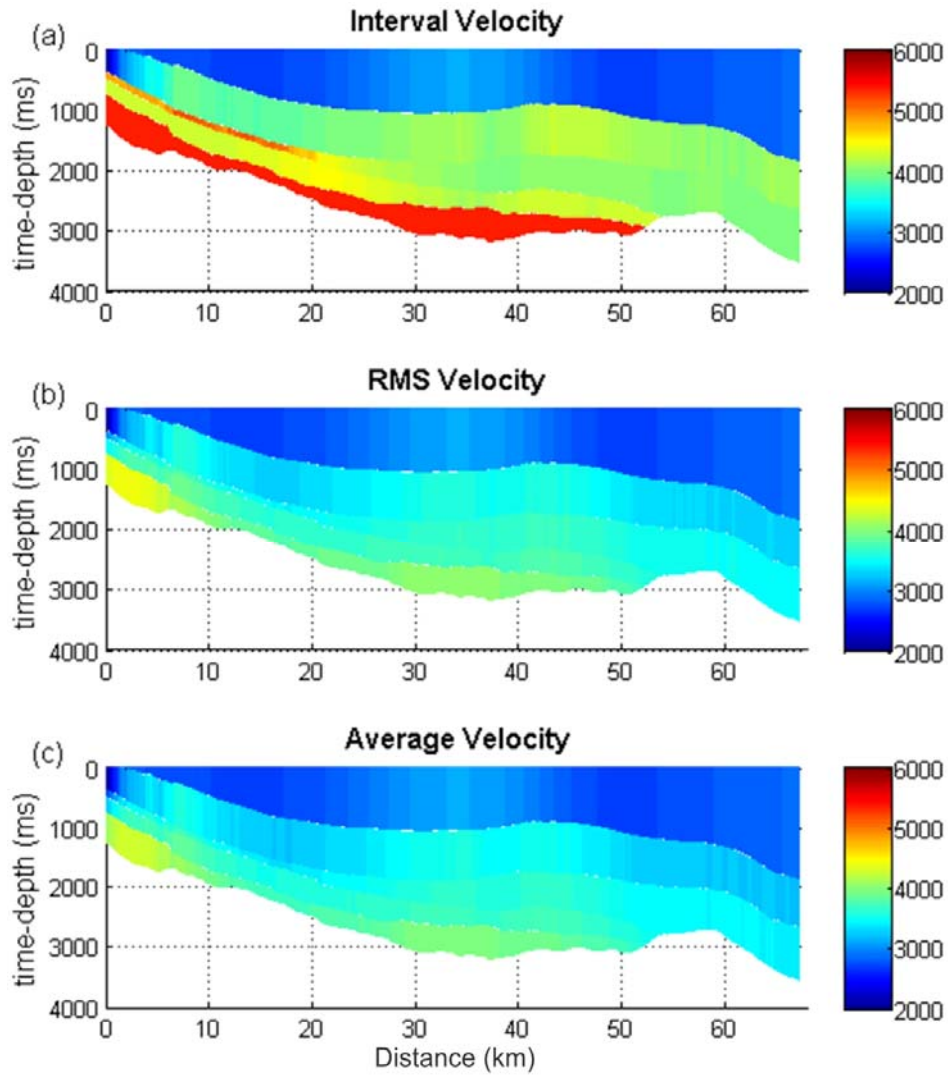


Figure 5. Time-distance plot of (a) interval, (b) RMS, and (c) average velocity models obtained by kriging with external drift. Color scale is the velocity in m s^{-1} .

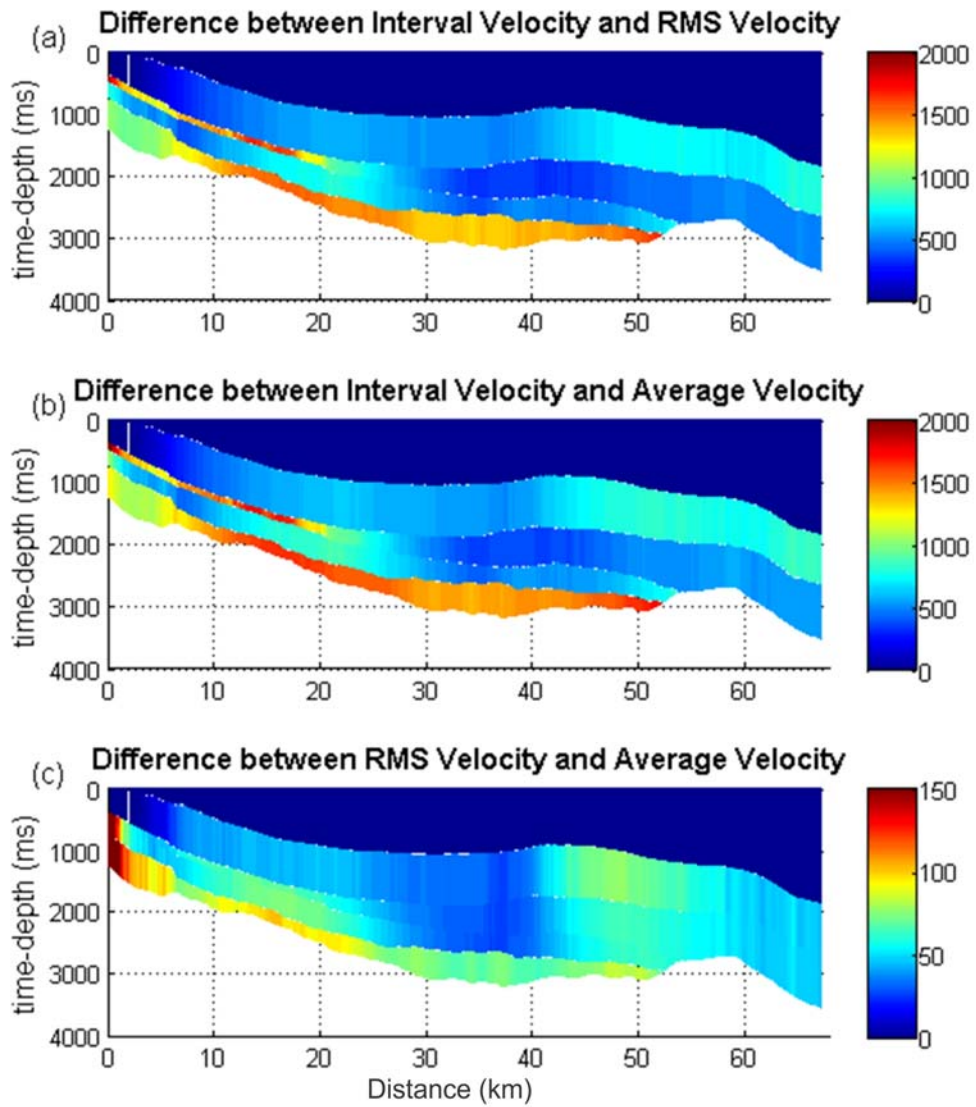


Figure 6. Time-distance plot of the velocity difference: (a) $V_{\text{int}} - V_{\text{rms}}$, (b) $V_{\text{int}} - V_{\text{ave}}$ and (c) $V_{\text{rms}} - V_{\text{ave}}$. Color scale is the velocity difference in m s^{-1} .

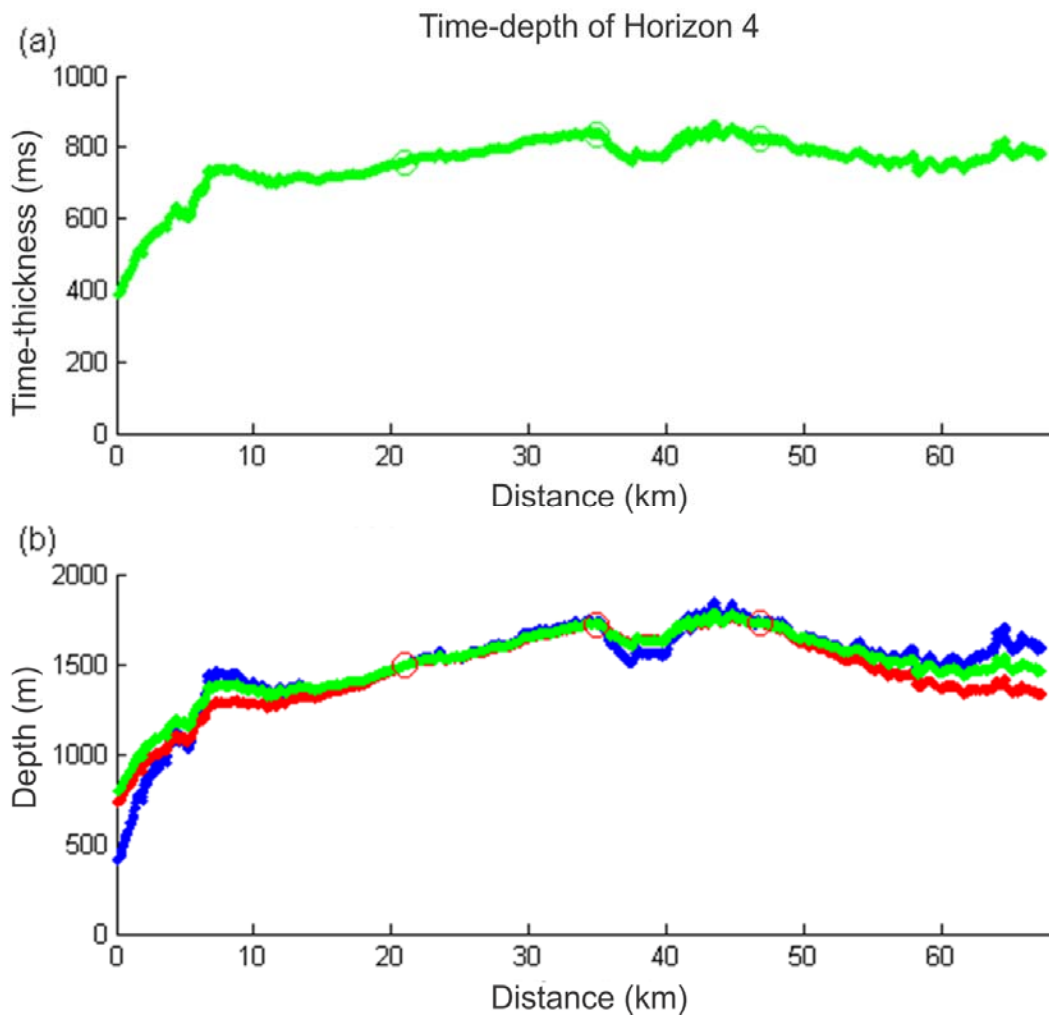


Figure 7. (a) Variations of time-depth with distance for horizon 4. (b) Variations of depth with distance of horizon 4 estimated by KED (blue curve) and CK with a coefficient of correlation of 0.8 (red curve) and 0.9 (green curve) between the primary and secondary variables.

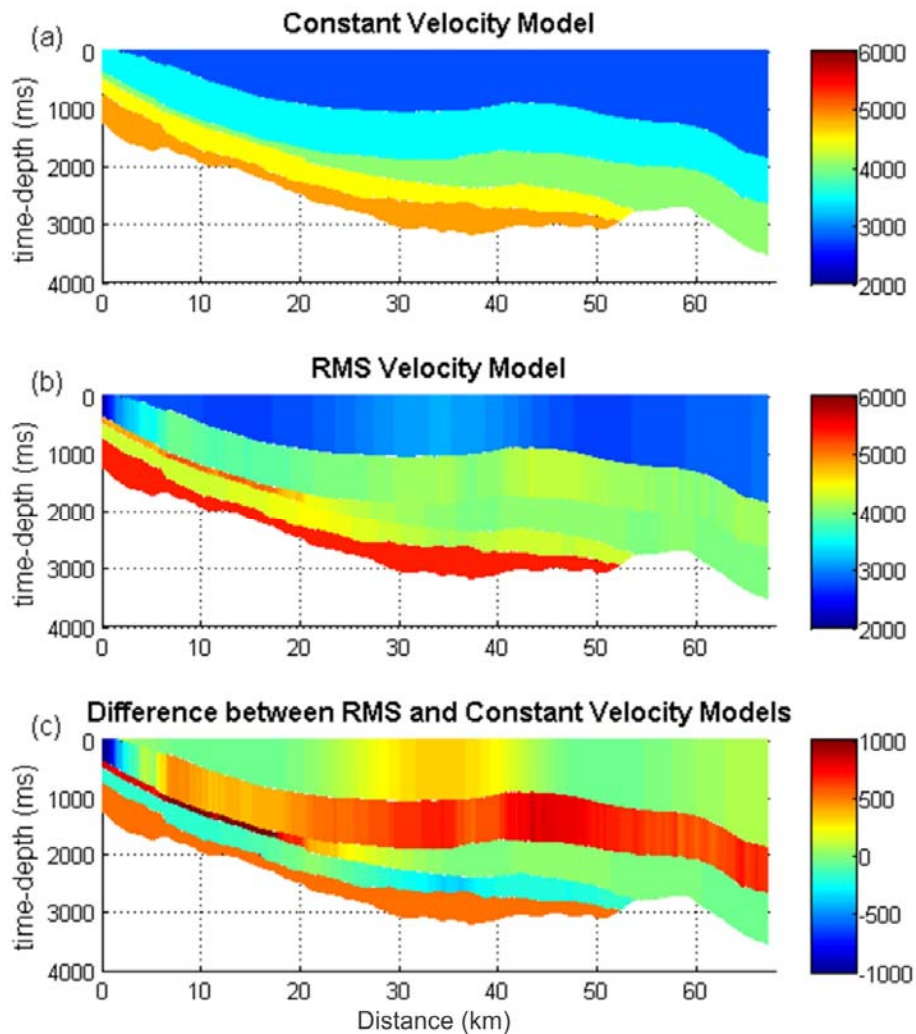


Figure 8. (a) Constant velocity layer model obtained by averaging RMS velocity calculated from well logs shown in figure 2. (b) RMS velocity model obtained by KED (same as figure 5b). (c) Time-distance plot of the velocity difference between the RMS and constant velocity models. Color scale is the velocity (a,b) and velocity difference (c) in m s^{-1} .

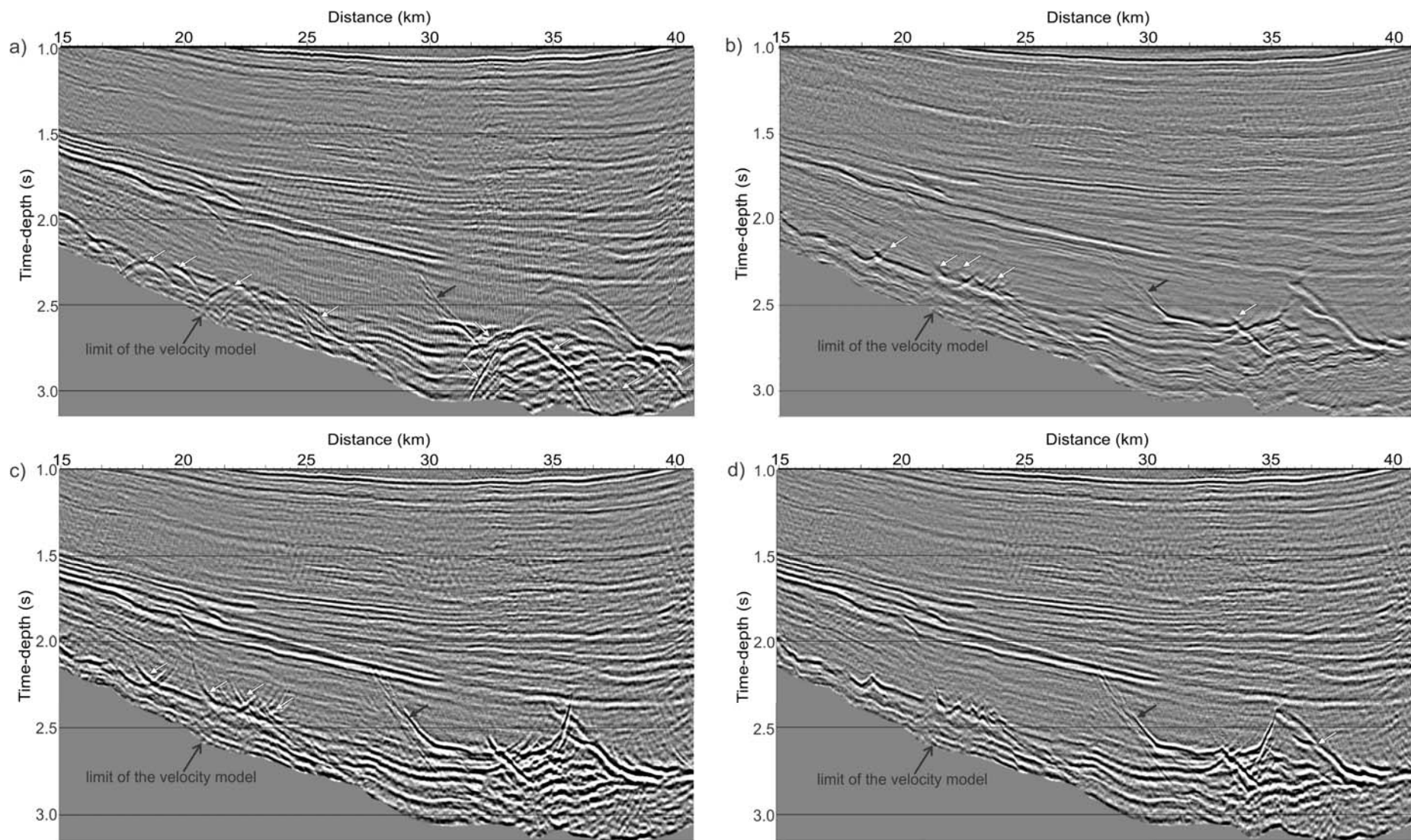


Figure 9. Enlarged portion of line 2674: (a) original stack, (b) post-stack Kirchhoff time-migration from Kanasewich and Berkes (1988), (c) post-stack Kirchhoff time-migration using the constant velocity layer model of figure 9a and (d) post-stack Kirchhoff time-migration using KED velocity model of figure 8(b). See figures 1 and 3 for location. For comparison data have been muted below the lower limit of the velocity models. Arrows are discussed in the text.